

## Supporting Information

### SI Figure Legends

**Figure S1: Quality and specificity control of Millipore 04-808 anti-H3R2me2a rabbit monoclonal antibody (mAb) using Active Motif's MODified Histone Peptide Array.**

Specificity analysis graph using the specificity factor as the ratio of the average intensity of all spots containing H3R2me2a divided by the average intensity of all spots not containing H3R2me2a.

**Figure S2: Regulation of PRMT6 and H3R2me2a 24 hr after repeated cocaine administration in the dorsal striatum (DS) and prefrontal cortex (PFC).** DS proteins levels of PRMT6 ( $t(18)=0.11$ ,  $p=0.91$ ), H3R2me2a ( $t(18)=0.34$ ,  $p=0.73$ ). PFC protein levels of PRMT6 ( $t(18)=0.39$ ,  $p=0.7$ ), H3R2me2a ( $t(18)=0.91$ ,  $p=0.38$ ). ( $n=10$ ). Data are presented as mean  $\pm$  SEM.

**Figure S3: Validation of viral vectors.** **i**, Tissue collection protocol after stereotaxic surgery with the respective viral vectors. **ii, iii**, HSV infected regions were dissected on day 3 after surgery and processed for RNA extraction as described in Methods with the respective RT-PCR human primers (hPRMT primers). Mice were injected intra-NAc with HSVs encoding the respective human constructs of PRMTs (HSV-hPRMT) 1, 5, 6, or 7 or HSV-GFP. **ii**, HSV-hPRMT1 injected NAc mRNA levels of hPRMT1 ( $t(8)=11.13$ ,  $p<0.0001$ ). HSV-hPRMT5 injected NAc mRNA levels of hPRMT5 ( $t(8)=21.11$ ,  $p<0.0001$ ). HSV-hPRMT6 injected NAc mRNA levels of hPRMT6 ( $t(8)=15.57$ ,  $p<0.0001$ ). HSV-hPRMT7 injected NAc mRNA levels of

hPRMT7 ( $t(8)=8.08$ ,  $p<0.0001$ ). ( $n=5$ ).  $**p<0.0001$  compared to HSV-GFP injected NAc. **iii**, HSV-hPRMT1 injected NAc mRNA levels of hPRMT1 primers:  $F(2,13)=161.4$ ,  $p<0.0001$ ; HSV-GFP vs HSV-hPRMT1:  $t(8)=16.93$   $p<0.0001$ . HSV-hPRMT6 injected NAc mRNA levels of hPRMT6 primers: hPRMT6 primers:  $F(2,14)=137.5$ ,  $p<0.0001$ ; HSV-GFP vs HSV-hPRMT6:  $t(8)=15.1$ . ( $n=4-5$ ).  $***p<0.0001$  vs HSV-GFP. **iv**, HSV-hPRMT6 or HSV-GFP infected regions were dissected on day 3 after surgery and processed for Western blotting as described in Methods. HSV-hPRMT6 infected NAc protein levels of PRMT6 ( $t(14)=2.501$ ,  $p=0.02$ ), H3R2me2a ( $t(9)=5.22$   $p=0.017$ ) vs HSV-GFP infected NAc. ( $n=4-8$ ).  $*p<0.05$ . **v**, AAV-PRMT6-miR or AAV-GFP infected regions were dissected on day 28 after surgery and processed for Western blotting as described in Methods. AAV-PRMT6-miR infected NAc protein levels of PRMT6 ( $t(16)=2.32$ ,  $p=0.03$ ) vs AAV-GFP infected NAc. ( $n=9$ ).  $*p<0.05$ . **vi**, HSV-GFP-LS1L-PRMT6 infected regions were dissected on day 3 after surgery and processed for Western blotting as described in Methods. HSV-GFP-LS1L-hPRMT6 infected NAc protein levels of PRMT6 in: D1-Cre + animals ( $t(7)=3.31$ ,  $p=0.01$ ) vs in D1-Cre -animals. ( $n=3-6$ ); D2-Cre + animals ( $t(16)=2.399$ ,  $p=0.029$ ) vs in D2-Cre -animals. ( $n=6-12$ ).  $*p<0.05$ . Data are presented as mean  $\pm$  SEM.

**Figure S4: Overexpression of PRMT1, 5, or 7 on cocaine CPP.** Upper panel- schematic of experiment. Lower panel- cocaine CPP with overexpression of PRMT1, 5, 7 or GFP HSV constructs in NAc.  $F(3,66)=0.49$ ;  $p=0.69$ . ( $n=7-27$ ).

**Figure S5: Cell-type specific regulation of PRMT6 in NAc. i. NAc *Prmt6* mRNA expression in D2-MSNs relative to D1-MSNs in saline treated animals.** D2-Cre-RiboTag mice NAc

mRNA levels fold change of *Prmt6* 24 hr after a 7 daily IP injections of saline vs D1-Cre-RiboTag mice. 24 hr after the last IP saline injection, *Prmt6* NAc mRNA levels: in D2-Cre-Ribotag line  $t(22)=1.36$ ,  $p=0.15$  compared to saline-treated D1-Cre-Ribotag mice; (n=11). **ii. Locomotor activity (30 min) in the CPP saline or cocaine (IP, 7.5 mg/kg) paired chambers with cell-type specific overexpression of PRMT6 in NAc infected with HSV-GFP-LS1L-PRMT6 in D1- or D2-Cre mice (Cre+) and in respective non Cre littermates (Cre-).** Upper panel- schematic for cocaine CPP, surgery, and locomotor testing with HSV-GFP-LS1L-PRMT6. Lower panel- cell-type specific overexpression of PRMT6 in D2-MSNs increases cocaine-induced locomotor activity. D1 line Saline:  $F(3,69)=1.03$ ;  $p=0.387$ ; D1 line Cocaine:  $F(3,69)=0.017$ ;  $p=0.99$  (n=17-18). D2 line Saline:  $F(3,87)=1.12$ ;  $p=0.35$ ; D2 line Cocaine:  $F(3,87)=6.34$ ;  $p=0.0006$ ; Day 1 cocaine: D2-Cre- vs D2-Cre:  $t(42)=3.0$ ;  $p<0.01$ ; Day 2: cocaine: D2-Cre vs D2-Cre +:  $t(42)=2.7$ ;  $p<0.05$ . \* $p<0.05$ , \*\* $p<0.01$ . Data are presented as mean  $\pm$  SEM.

**Figure S6: *Srcin1* structure and H3R2me2a and H3K4me3 ChIP-seq coverage (reads per million mapped reads) after repeated cocaine at specific loci. i,** *Srcin1* in mouse ('p', promoter; 'e', exon; 'i', intron) is located on chromosome 11, composed of 20 exons and is 69kb long. **ii,** Integrative Genomics Viewer (IGV) track views of H3R2me2a and H3K4me3 ChIP-Seq peaks at *Srcin1* promoter (green, a) and at *Srcin1* intron1-2 (centered on diffRep in yellow, b) under saline (blue) and repeated cocaine conditions (red). IGV 2.3 (Broad Institute) was used for visualization of all ChIP-seq tracks.

**Figure S7: H3R2me2a genome-wide ChIP-seq read distribution in saline and cocaine conditions.** Pie charts showing H3R2me2a peaks for several genomic features reveals that the

large majority of H3R2me2a peaks reside in both intergenic and genic regions, with ~35% associated with introns. A small number of peaks reside within exons and promoters. No significant differences in peak distribution between saline- and cocaine-treated (24 hr) animals were observed. Cocaine induced 320 H3R2me2a peaks, with saline showing 87 peaks.

**Figure S8: Cocaine induction of Srcin1 in NAc is blocked by overexpression of PRMT6.**

HSV infected regions were dissected and processed for Western blotting as described. HSV-GFP sal vs coc:  $t(17)=3.97$ ,  $p<0.01$ ; HSV-GFP coc vs HSV-PRMT6 coc:  $t(19)=4.18$ ,  $p<0.001$ . (n=8-10). \* $p<0.01$  and \*\*  $p<0.001$ . Data are presented as mean  $\pm$  SEM.

**Figure S9: Validation of HSV-Srcin1 overexpression *in vivo*.** HSV infected regions were dissected and processed for Western blotting as described. HSV-Srcin1:  $t(10)=2.97$ ,  $p=0.01$  vs HSV-GFP. (n=6). \* $p<0.05$ . Data are presented as mean  $\pm$  SEM.

**Figure S10: Validation of HSV-GFP-LS1L-Srcin1 overexpression *in vivo*.**

HSV-GFP-LS1L-Srcin1 infected regions were dissected on day 3 after surgery and processed for Western blotting as described in Methods. HSV-GFP-LS1L-Srcin1 infected NAc protein levels of Srcin1 in: D1-Cre+ animals ( $t(6)=2.75$ ,  $p=0.04$ ) vs in D1-Cre- animals. (n=6-8); D2-Cre+ animals ( $t(12)=3.13$ ,  $p=0.016$ ) vs in D2-Cre- animals. (n=8-12). \* $p<0.05$ . Data are presented as mean  $\pm$  SEM.

## **SI List of Tables:**

### **Table S1: H3R2me2a ChIP-seq library quality control.**

ChIP-seq data were aligned to the mouse genome (mm9) by CASAVA 1.8

([http://www.illumina.com/software/genome\\_analyzer\\_software.ilmn](http://www.illumina.com/software/genome_analyzer_software.ilmn)), and only unique reads

were retained for analysis by ELAND. FastQC

(<http://www.bioinformatics.babraham.ac.uk/projects/fastqc/>) was applied for quality control, and

then SAMTools (<http://samtools.sourceforge.net>) was used to remove potential PCR duplicates

(1). PhantomPeak (<https://code.google.com/p/phantompeakqualtools/>) was applied to estimate

the quality and enrichment (NSC and RSC) of the ChIP-seq dataset (2).

### **Table S2: List of qPCR primers.**

### **Table S3: List of antibodies.**

### **Table Data Set S1: H3R2me2a ChIP-seq peak list in saline and cocaine conditions.**

The chromosomal locations of these sites are shown in the Table as Start to Finish, and annotated to the genome accordingly.

### **Table Data Set S2: List of cocaine-induced changes from H3R2me2a ChIP-seq using**

**diffReps.** Binding up: differential binding sites increased after cocaine; Binding down:

differential binding sites decreased after cocaine. A false discovery rate (FDR) cutoff of <10%

was used to choose the sites that are significant. The chromosomal locations of these sites are shown in the Table as Start to Finish, and annotated to the genome accordingly.

## SI Methods

**Animals and treatments:** For all experiments, 7 to 9-week-old C57BL/6J male mice (25-30 g; The Jackson Laboratory, Bar Harbor, ME, USA) were housed five per cage in a colony room set at constant temperature (23°C) on a 12 hr light/dark cycle (lights on from 0700 to 1900 hr) with *ad libitum* access to food and water. D1-Cre and D2-Cre male mice, fully backcrossed to a C57BL/6J background, were also used for some experiments as described; wildtype littermates were used as controls. The RiboTag mouse (HA-Rpl22) from The Jackson Laboratory was crossed to the D1- or D2-Cre-expressing mouse which results in the HA-tag being expressed only in cells that express Cre (D1-Cre-Ribotag or D2-Cre-Ribotag mouse lines). D1-Cre-RiboTag and D2-Cre-RiboTag mice, also on a C57BL/6J background, were used for cell-type specific analysis of gene expression. Male Sprague Dawley rats (250–275 g; Charles River Laboratories) were pair-housed in a similar climate-controlled room on a 12 hr reverse light/dark cycle (lights off at 0700) with access to food and water *ad libitum*. All animals were habituated for at least 1 week before experimentation. All animal protocols were approved by the Institutional Animal Care and Use Committee (IACUC) at Mount Sinai, University at Buffalo, and University of Maryland. For all experiments, extensive laboratory experience and data from preliminary investigations were used to estimate required sample sizes. Animals were randomly assigned to experimental groups to which experimenters were blinded. For repeated cocaine treatment, animals received daily intraperitoneal (IP) injections for seven consecutive days of cocaine (Sigma-Aldrich, St. Louis, MO, USA) at 20 mg/kg body weight ('repeated cocaine'). Mice were used 24 hr after the final injection. For acute cocaine treatment, mice received only

one injection of cocaine at 20 mg/kg body weight on day seven after six daily IP saline injections. Control mice for all groups received daily saline injections for seven days.

**NAc RNA isolation and qRT-PCR:** Bilateral 14-gauge punches of mouse NAc were obtained 24 hr after the last cocaine injection and frozen on dry ice. Each sample contained bilateral 14-gauge NAc punches from a single animal. Samples were then homogenized in TRIzol and processed according to manufacturer's instructions (Life technologies, NY, USA). RNA was purified with RNAeasy Micro columns (Qiagen, CA, USA) and reverse transcribed into cDNA using an iScript DNA synthesis Kit (BioRad, CA, USA). cDNA was quantified by qPCR using SYBR green. Each reaction was performed in duplicate and analyzed following the standard  $\Delta\Delta C_t$  method using glyceraldehyde-3-phosphate dehydrogenase (GAPDH) as a normalization control. Primers were designed to flank exon/intron boundaries and were created using the open-source software Primer3 (SI Appendix, Table S2). BLAST and dissociation curve analysis were also performed to ensure specificity of primer design.

**Western blotting:** Frozen NAc, dorsal striatum (DS), and medial prefrontal cortex (PFC) tissue from individual animals was homogenized in 30  $\mu$ l of homogenization buffer containing 320 mM sucrose, 5 mM HEPES buffer, 1% SDS, phosphatase inhibitor cocktails I and II (Sigma St. Louis, MO, USA), and protease inhibitors (Roche, Basel, Switzerland) using an ultrasonic processor (Cole Parmer, Vernon Hills, Illinois, USA). Protein concentrations were determined using a DC protein assay (Bio-Rad, Hercules, CA, USA), and 10-30  $\mu$ g of protein were loaded onto 4-15% or 18% gradient Tris-HCl polyacrylamide gels for electrophoresis fractionation (Bio-Rad). Proteins were transferred to nitrocellulose membranes, incubated for 1 hr at room



temperature (RT) in 5% of bovine serum albumin (BSA) blocking buffer, and incubated overnight at 4°C with primary antibodies (SI Appendix, Table S3) diluted in 5% BSA blocking buffer. After thorough washing with 1x Tris-buffered saline plus 0.1% Tween-20 (TBS-T), membranes were incubated with respective HRP-conjugated secondary antibodies (1:50000, Vector, Burlingame, CA) dissolved in 5% BSA for 1 hr at room temperature. For ECL analysis, immunoreaction was detected using an enhanced chemiluminescence system (Pierce Biotechnology - Thermo Fisher Scientific, Rockford, IL). Resulting blots were quantified by densitometry using NIH ImageJ (NIH, Bethesda, Maryland, USA). Data were normalized to levels of GAPDH, actin, or total H3, which were not affected by cocaine treatment.

**Human postmortem brain tissue:** NAc tissue, obtained from the Quebec Suicide Brain Bank (IRB approval from Douglas Mental Health Institute at McGill University, Montreal, Quebec, Canada) was analyzed for control and cocaine-addicted subjects matched for age, postmortem interval, RNA integrity, and pH. Standard dissection technique was used and the tissue was snapped frozen and stored at -80°C. Please see ref (3) for further details of the demographic characteristics of these patients and quality measures of their brains.

**Generation of viral constructs:** Human *PRMT1*, 5, 6, and 7 pcDNA3 plasmids were obtained from Dr. Fabio Casadio (Rockefeller University NY) and cloned into HSV vectors. Briefly, *PRMT1* and *PRMT6* pcDNA3 plasmids were first cloned into HSV p1005+ by excising them with KpnI (5') and EcoRI (3') from their original vector and cloning them into HSV p1005+ with the same enzymes. *PRMT5* pcDNA3 plasmid was excised using BamHI (5') and EcoRI (3') and *PRMT7* with XhoI (5') and EcoRI (3'). Gateway cloning technology (Invitrogen) was then

used to recombine *PRMT6* into a Cre-inducible loxP-STOP-loxP HSV p1006 (HSV-GFP-LS1L-PRMT6). *Srcin1* (p140Cap) was cloned into the HSV p1005+ vector using PCR-based cloning. All HSV vectors, which expressed GFP in addition to designated transgenes, were packaged into high-titer viral particles (between  $3-4 \times 10^8$  particles/ml) as described previously (4).

**Viral-mediated gene transfer:** Mice were positioned in small animal stereotaxic instruments, under ketamine anesthesia, and their cranial surfaces were exposed. Thirty-three gauge syringe needles were bilaterally lowered into NAc to infuse 0.5  $\mu$ l of virus at a 10° angle (anterior/posterior (A/P), + 1.6 mm; medial/lateral (M/L), + 1.5 mm; dorsal/ventral (D/V), - 4.4 mm from Bregma). Infusions occurred at a rate of 0.1  $\mu$ l/min. Animals receiving HSV injections were allowed to recover for at least 24 hr following surgery.

**Immunoprecipitation of polyribosomes and RNA isolation from MSN subtypes:** Immunoprecipitation of polyribosomes was performed on NAc of D1-Cre-RiboTag and D2-Cre-RiboTag mice (5). In brief, four 14-gauge NAc punches per animal (four animals pooled per sample) were collected and homogenized by douncing in homogenization buffer containing Tris 50 mM (pH 7.4), KCl 100 mM, MgCl<sub>2</sub> 12 mM, and NP-40 1% supplemented with DTT 1 mM, cycloheximide 100  $\mu$ g/mL, heparin 1 mg/mL, and RNAase and protein inhibitors (Promega; Roche). Samples were then centrifuged at 10,000 x g for 10 min to collect clear supernatants. 80  $\mu$ l of supernatant was transferred to new tubes to serve as input for sample validation and 800  $\mu$ l of the supernatant was added directly to HA-coupled beads (Invitrogen: 100.03D; Covance: MMS-101R) for constant rotation overnight at 4°C. The following day, magnetic beads were washed three times in magnet for 5 min in high salt buffer (Tris 50 mM (pH 7.4), KCl 300 mM,

MgCl<sub>2</sub> 12 mM, NP-40 1%, DTT 1 mM, and cycloheximide 100 µg/ml). Finally, RNA was extracted by adding TRK lysis buffer to the pellet provided in MicroElute Total RNA Kit (Omega) according to manufacturer's instructions. RBA was quantified with a NanoDrop (Thermo Scientific). RNA integrity was measured using the Agilent 2100 Bioanalyzer at the Biopolymer/Genomics Core Facility at University of Maryland.

**Conditioned place preference:** We used an unbiased CPP paradigm, similar to one used in previous studies to examine the effect of PRMTs and Srcin1 on cocaine reward. Mice were conditioned for two days to saline injections (IP) in one chamber for 30 min during a morning session (AM) and to cocaine injections (7.5 mg/kg IP) to the opposite chamber for 30 min during an afternoon session (PM). The day after the second conditioning, mice were tested for place preferences during a 20-min session where they were allowed to freely explore all chambers. The CPP score represented the difference in the time spent in seconds between the cocaine and the saline paired chambers.

**Self-administration of cocaine:** Rats were implanted with chronic indwelling intra-jugular catheters and trained for self-administration as described respectively in in Fig. 4 (6). Briefly in Fig.4, rats were trained to self-administer cocaine (0.8 mg/kg/infusion) for 2 hr sessions until acquisition criteria were met (2 days, >20 injections, 70% responses on active lever). The NAc was then injected bilaterally (as above) with either HSV-GFP or HSV-Srcin1 equally counterbalanced for performance. On day 2-5 of viral expression, the threshold procedure was used to determine changes in the reinforcing efficacy of cocaine. In each single session, rats were given access to a descending series of 11 unit doses of cocaine (421, 237, 133, 75, 41, 24, 13,

7.5, 4.1, 2.4, 1.3,  $\mu\text{g}/\text{injection}$ ) on an FR1 schedule during consecutive 10-min bins within a daily session. This was performed for 3 consecutive days and the average was taken. Behavioral economic analysis was used to determine the parameters of maximal price paid ( $P_{\text{max}}$ ), as described previously (7, 8).

**ChIP, library preparation, and sequencing:** 3 fully independent biological replicates for saline and for cocaine treatment were obtained for H3R2me2a. For each ChIP-seq replicate, bilateral 14-gauge NAc punches were pooled from 10 mice. Tissue was lightly fixed to cross-link DNA with associated proteins, and the material was further sheared (Bioruptor to obtain mostly 100-300 bps fragments) and immunoprecipitated using sheep anti-rabbit magnetic beads (Invitrogen) conjugated to an antibody that specifically recognizes H3R2me2a (Millipore 04-808) and which we validated extensively (SI Appendix, Fig. S2). Immunoprecipitated DNA and total (input) genomic DNA were prepared for ChIP-seq using an Illumina kit according to the manufacturer's instructions. Each sample underwent end repair followed by addition of an A base to the 3' end. Proprietary adapters were then ligated to the ends, followed by size selection on a 2% agarose gel. The range of excision was 200–300 bp. After DNA clean up, samples were amplified with 21 cycles of PCR. Amplification and size selection were confirmed with a BioAnalyzer. The resulting libraries were sequenced on an Illumina HiSeq 2500 with 100 bp read length.

**ChIP-seq data analysis:** ChIP-seq data were aligned to the mouse genome (mm9) by CASAVA 1.8 ([http://www.illumina.com/software/genome\\_analyzer\\_software.ilmn](http://www.illumina.com/software/genome_analyzer_software.ilmn)), and only unique reads were retained for analysis. FastQC (<http://www.bioinformatics.babraham.ac.uk/projects/fastqc/>) was applied for quality control, and then SAMTools (<http://samtools.sourceforge.net>) was used

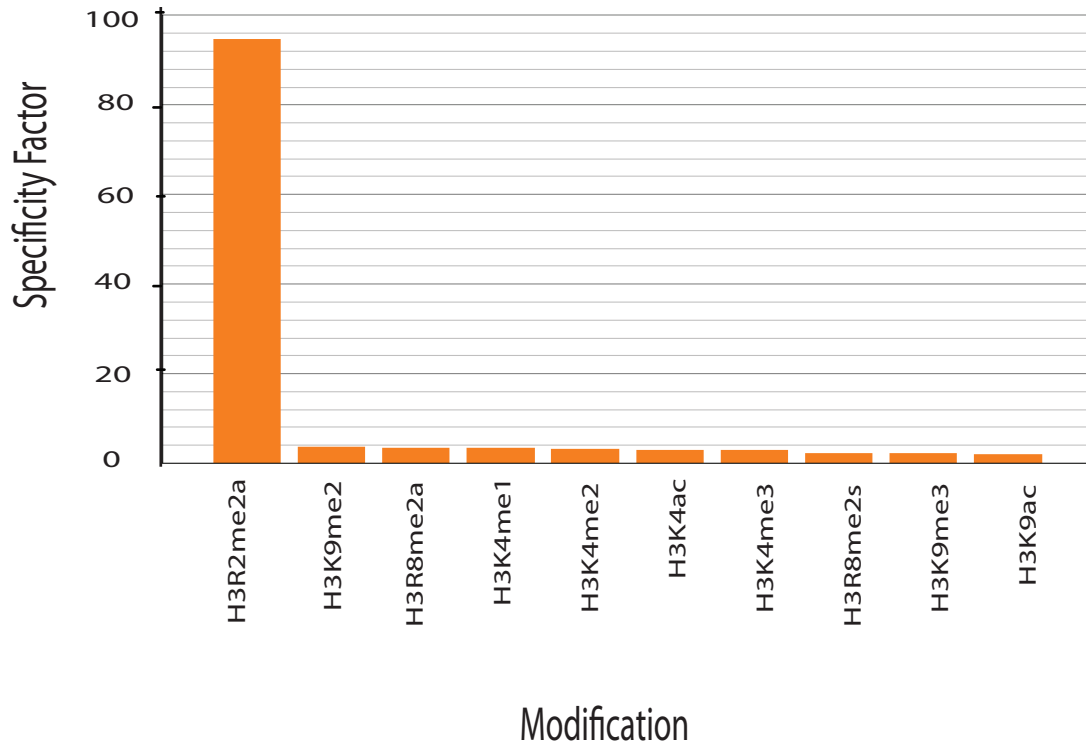
to remove potential PCR duplicates (1). PhantomPeak (<https://code.google.com/p/phantompeakqualtools/>) was applied to estimate the quality and enrichment of the ChIP-seq datasets (2). Additional ENCODE quality metrics, such as the normalized strand coefficient (NSC) and the relative strand correlation (RSC), were calculated (9). For all samples,  $NSC \geq 1.03$  and  $RSC \geq 0.8$  (SI Appendix, Table S1). All 3 replicates of each condition were pooled and normalized to 1 million reads. The density of H3R2me2a binding 1 to 2 kb up- and downstream of TSSs of coding genes in Ensembl annotations were plotted. diffReps was used to compare the differential enrichment of H3R2me2a between saline and cocaine treated mice. The Corrgram package in R software (<http://www.r-project.org/>) was used to calculate and visualize the correlation between H3R2me2a and other histone marks from published datasets (10). TDF files (with all duplicative/redundant reads  $>2$  removed) were applied in IGV for genome browser views of ChIP-seq tracks.

**Statistical analysis:** Numerical analyses were performed using GraphPad Prism version 5.0 for Windows, GraphPad Software, La Jolla California USA. Student's t-tests were used whenever two groups were compared, while one-way analysis of variance (ANOVA) was performed to determine significance for all other data (except ChIP-seq findings) (Fig. 1a, SI Appendix, Fig. S3iii). Significant main effects ( $p < 0.05$ ) were further analyzed using post hoc tests. For Fig. 1b,c, we designated parameters that were significant after the Bonferroni's correction for 9 indices ( $\#p < 0.05$ ;  $*p < 0.006$ ). All other analyses were based on correlated variables or stated explicit hypotheses and were therefore not corrected for multiple testing after student t-tests (11, 12).

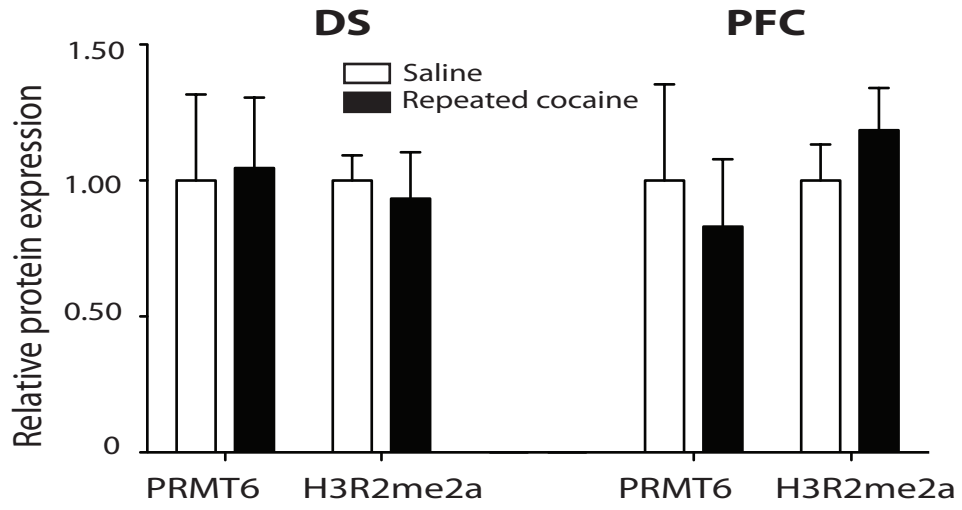
## SI References

1. Shen L, Shao N, Liu X, & Nestler E (2014) ngs.plot: Quick mining and visualization of next-generation sequencing data by integrating genomic databases. *BMC Genomics* 15:284.
2. Landt SG, *et al.* (2012) ChIP-seq guidelines and practices of the ENCODE and modENCODE consortia. *Genome Res* 22(9):1813-1831.
3. Robison AJ, *et al.* (2013) Behavioral and structural responses to chronic cocaine require a feedforward loop involving DeltaFosB and calcium/calmodulin-dependent protein kinase II in the nucleus accumbens shell. *The Journal of neuroscience : the official journal of the Society for Neuroscience* 33(10):4295-4307.
4. Grueter BA, Robison AJ, Neve RL, Nestler EJ, & Malenka RC (2013) FosB differentially modulates nucleus accumbens direct and indirect pathway function. *Proceedings of the National Academy of Sciences of the United States of America* 110(5):1923-1928.
5. Sanz E, *et al.* (2009) Cell-type-specific isolation of ribosome-associated mRNA from complex tissues. *Proceedings of the National Academy of Sciences of the United States of America* 106(33):13939-13944.
6. Calipari ES, Ferris MJ, Salahpour A, Caron MG, & Jones SR (2013) Methylphenidate amplifies the potency and reinforcing effects of amphetamines by increasing dopamine transporter expression. *Nature communications* 4:2720.
7. Oleson EB & Roberts DC (2012) Cocaine self-administration in rats: threshold procedures. *Methods Mol Biol* 829:303-319.
8. Bentzley BS, Fender KM, & Aston-Jones G (2013) The behavioral economics of drug self-administration: a review and new analytical approach for within-session procedures. *Psychopharmacology* 226(1):113-125.
9. Shen L, Choi I, Nestler EJ, & Won KJ (2013) Human Transcriptome and Chromatin Modifications: An ENCODE Perspective. *Genomics Inform* 11(2):60-67.
10. Feng J, *et al.* (2014) Chronic cocaine-regulated epigenomic changes in mouse nucleus accumbens. *Genome biology* 15(4):R65.
11. Feise RJ (2002) Do multiple outcome measures require p-value adjustment? *BMC Med Res Methodol* 2:8.
12. Streiner DL & Norman GR (2011) Correction for multiple testing: is there a resolution? *Chest* 140(1):16-18.

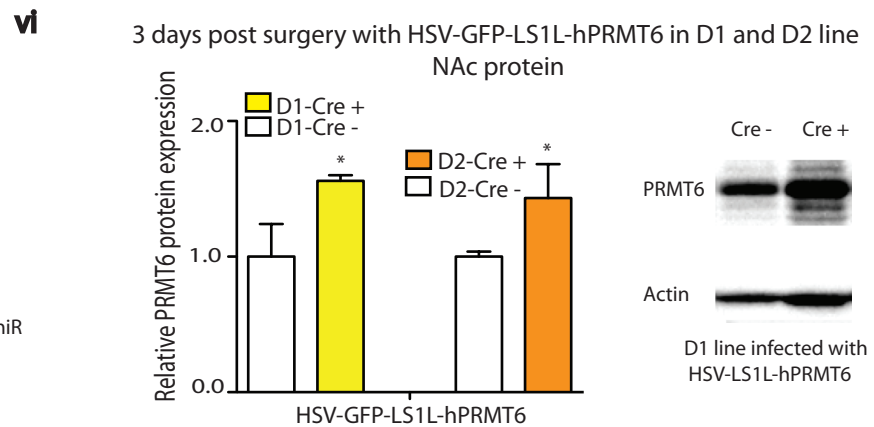
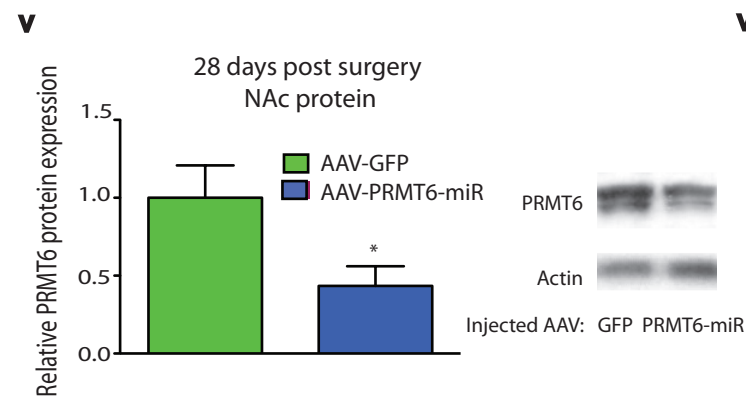
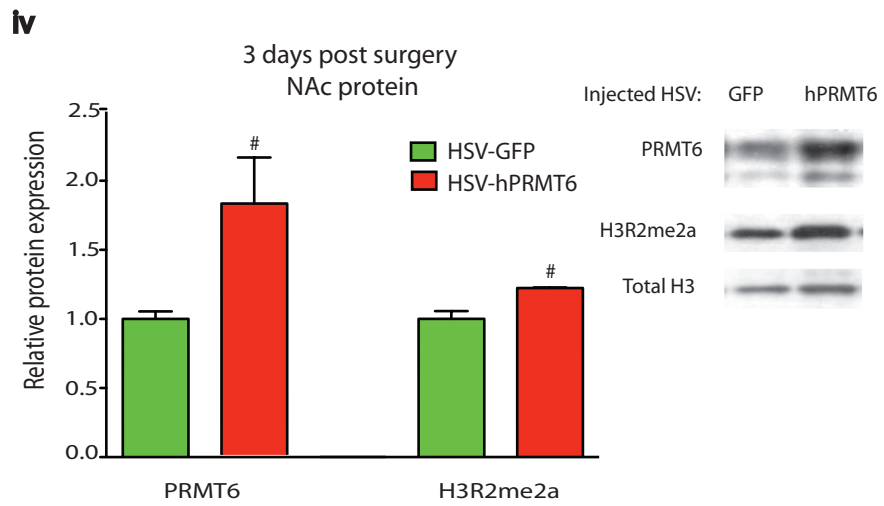
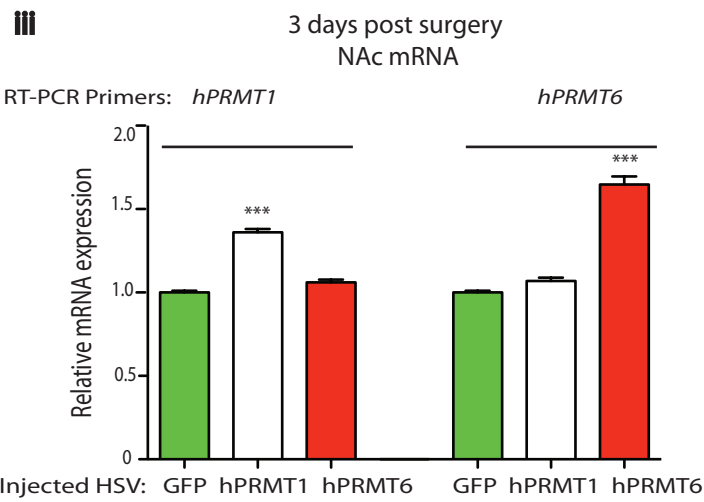
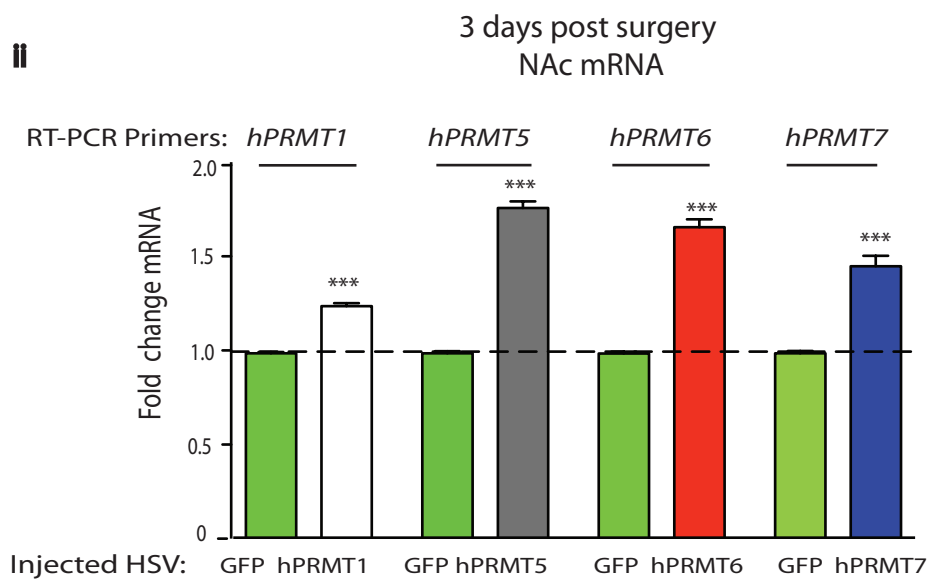
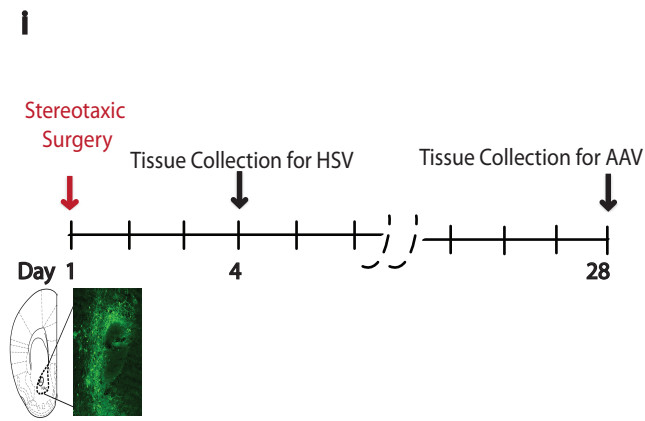
Specificity Analysis Graph for Millipore 04-808 H3R2me2a rabbit mAb

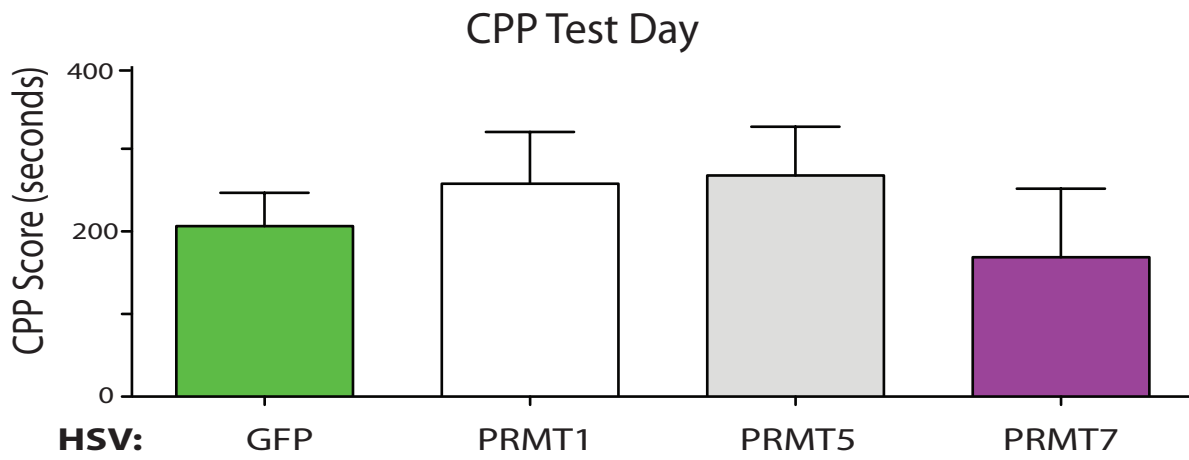
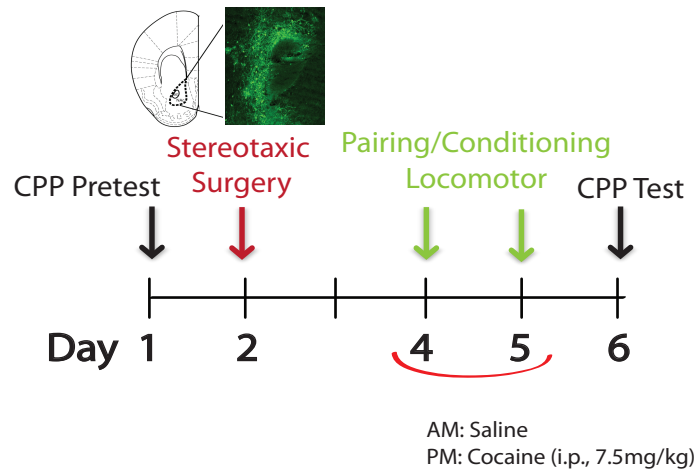


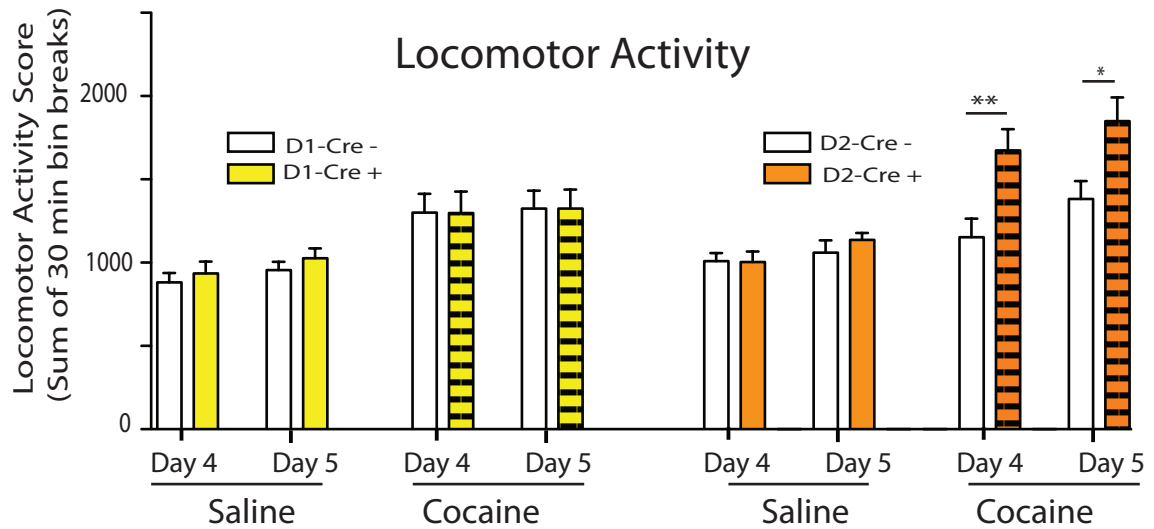
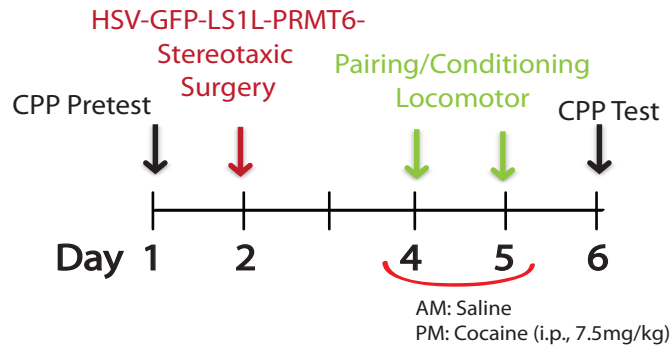
## 24 hours post Protein levels



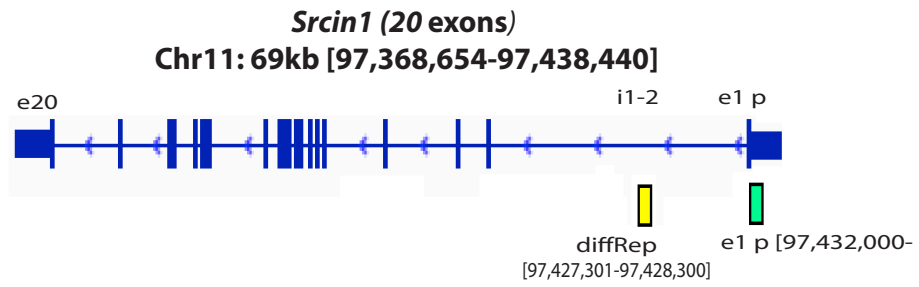








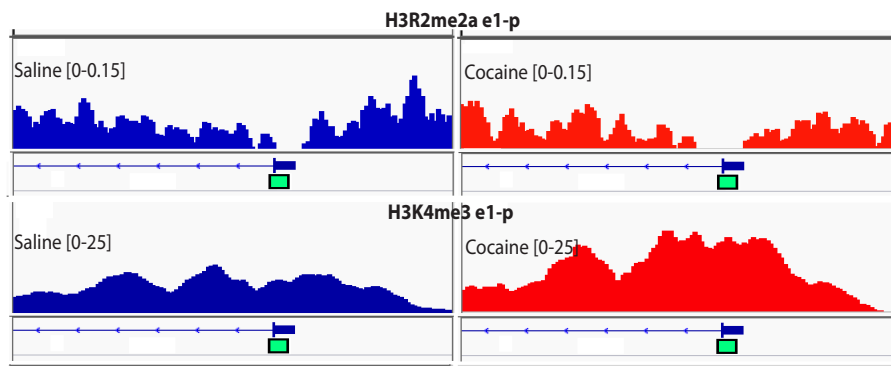
i



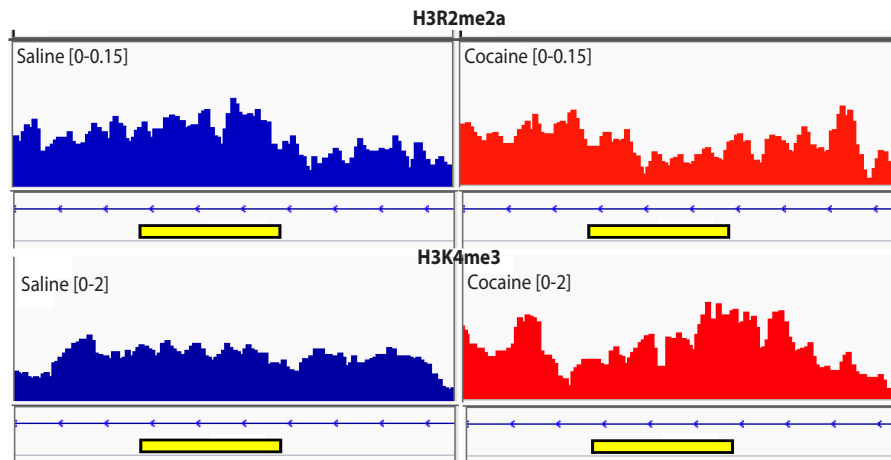
ii

Normalized genome coverage for H3R2me2a and H3K4me3 around *Srcin1* promoter(a) and *Srcin1* intron 1-2 (b)  
(reads per million mapped reads)

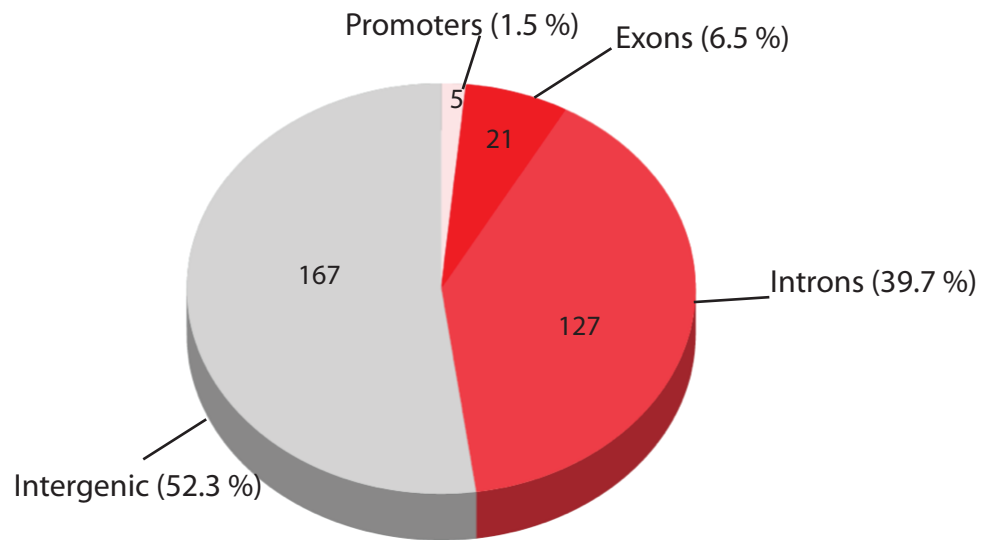
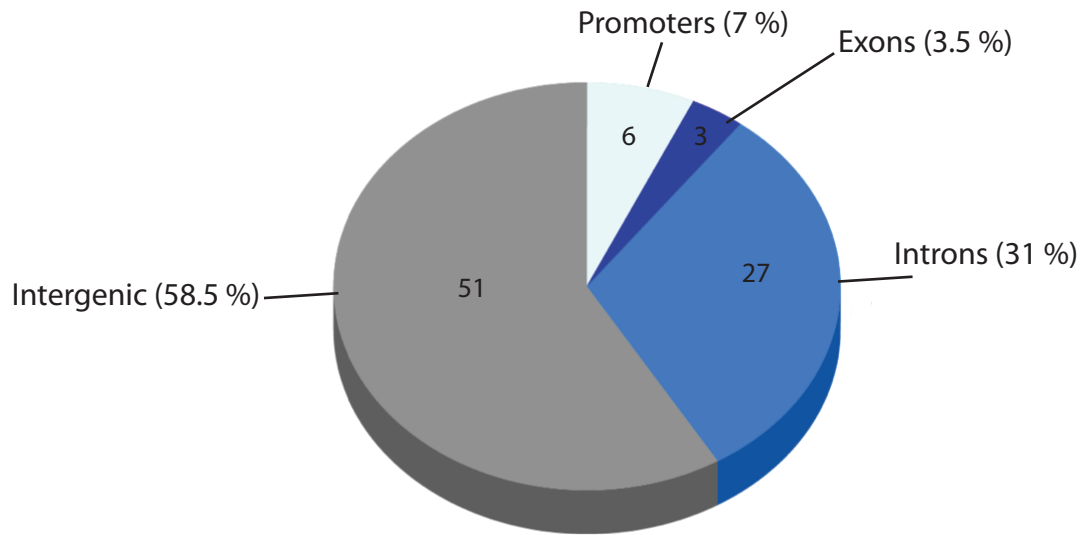
a. Around *Srcin1* exon1 -promoter [97,432,000-97,438,000]:



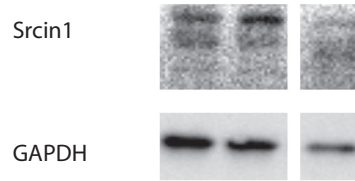
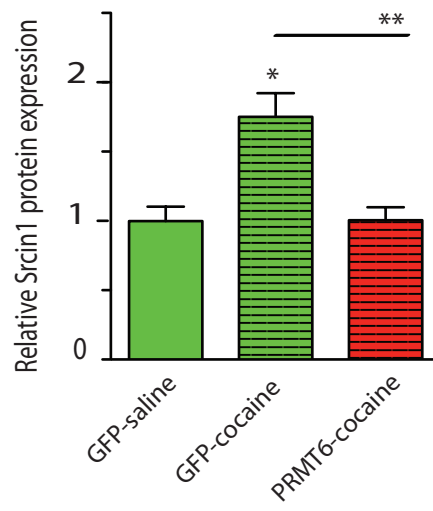
b. Around *Srcin1* intron1-2 [97,425,000-97,429,000]:



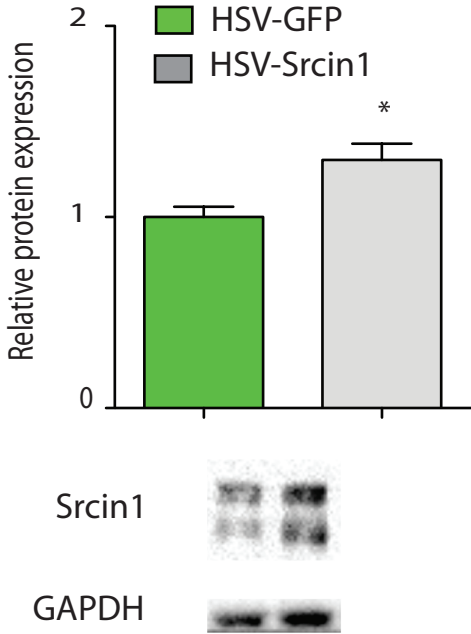
H3R2me2a ChIP-seq peak distribution genome-wide after saline and repeated cocaine

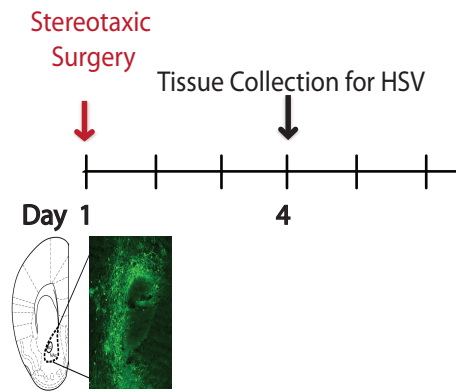


Srcin1 protein in HSV-GFP and HSV-PRMT6 infused NAc

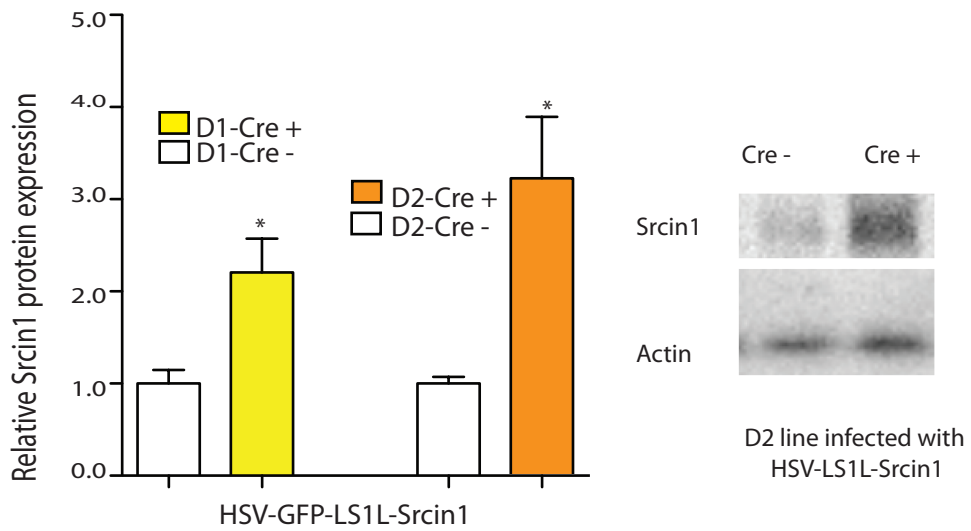


# Validation of HSV-Srcin1 overexpression in vivo





3 days post surgery with HSV-GFP-LS1L-Srcin1 in D1 and D2 line  
 NAc protein





## Quality control for H3R2me2a ChIP-seq library

Sample ID	Total raw reads	Uniquely mapped reads	Reads after deduplication	Total reads		NSC	RSC
Input Saline	124649719	95973733	28675986			1.09	8.22
Input Cocaine	134190846	94086291	40104555			1.06	8.75
Sal1 H3R2me2a	124557459	70375973	54181486			1.04	6.81
Sal1 H3R2me2a	138462499	83033848	55428651			1.05	5.21
Sal1 H3R2me2a	140068406	95286035	44782371	Saline:	154392508	1.05	7.07
Coc1 H3R2me2a	126729504	94648983	32080521			1.07	6.85
Coc2 H3R2me2a	132760811	50214095	82546716			1.03	3.50
Coc3 H3R2me2a	120222095	70349409	49872686	Cocaine:	164499923	1.05	5.26

## Human RT-PCR primers

*Prmt1 F* TCA TAA AGG AGG TGG ACA TCT ATA C  
*Prmt1 R* CTC TTG TGG CAG CGT GTG  
*Prmt5 F* TGC AGT GGC TCT TGA AAT TG  
*Prmt5 R* TGG TGC CTG TGA TGA TGA AC  
*Prmt6 F* GGG AAC TGA AGA GGA AGA TGG  
*Prmt6 R* GAA GGA TAC CCA GGC GGT AG  
*Prmt7 F* GCT GTG GTT GTG GAG TTC AG  
*Prmt7 R* GCT GCT GGA AGT CAA AGG TC

## Rat RT-PCR primers

*18S F* GGA TCC ATT GGA GGG CAA GT  
*18S R* ACG AGC TTT TTA ACT GCA GCA A  
*Prmt1 F* CAT GTT TCA CAA TCG GCA TC  
*Prmt1 R* ATG TCC ACC TTC TCC ACA GG  
*Prmt4 F* ACC ACA CCG ACT TCA AGG AC  
*Prmt4 R* CCT CTA CTT TGC CAG GGA TG  
*Prmt5 F* TGA GGC ACA GTT TGA GAT GC  
*Prmt5 R* TCA CCT CCA CAG GAA ACT CC  
*Prmt6 F* CCG GCA TTC TTA GCA TCT TC  
*Prmt6 R* TAG CCC ATC CAC TCG CTT AC  
*Prmt7 F* CTG CCT TTG TGT GAG TGA CG  
*Prmt7 R* AAA GGT TCA CCC AGG AGG AG

## Mouse RT-PCR primers

*18S F* CAG AAG GAC GTG AAG GAT GG  
*18S R* CAG TGG TCT TGG TGT GCT GA  
*Actin F* GCT TCT TTG CAG CTC CTT CGT  
*Actin R* CCA GCG CAG CGA TAT CG  
*Cobll1 F* TTT GGA AGA TGG GAT TGC TC  
*Cobll1 R* ACA CCA GAG GTC AAG GAT GC  
*Exoc6 F* GCT GGC TGA TTA TGA CTG GAC  
*Exoc6 R* AAG GAT GTG GAC AGA TGT TGG  
*Fryl F* GGA TAA CCC GCC CTA CTA CC  
*Fryl R* AGC TGC TAC TGT ATC GGG AC  
*Gapdh F* AAC GAC CCC TTC ATT GAC  
*Gapdh R* TCC ACG ACA TAC TCA GCA C

## Mouse RT-PCR primers

*Mllt3 F* GCT CCA CAG AAG GTT AAT GAC AC  
*Mllt3 R* GGA TGT TCC AGA TGT TTC CAG  
*Mxd1 F* AAG CCG ACA CAC CAC TCT G  
*Mxd1 R* CTG TCC ATC CGA GTC CTC TC  
*Prmt1 F* GCC TGC AAG TGA AGA GGA AC  
*Prmt1 R* CAA AGA TCT CCT CGC CAG TC  
*Prmt2 F* AGG CTG CTG TGG TTA CAT CC  
*Prmt2 R* TGA CGC TGT GGT ACT TGG TG  
*Prmt3 F* GTC AGA ACC TGC TCC TCC AC  
*Prmt3 R* ATT CCA GTT CCA CAC CCA AC  
*Prmt4 F* CAC CCC ACG ATT TCT GTT CT  
*Prmt4 R* TCT GTC CGC TCA CTG AAC AC  
*Prmt5 F* CTG AGT GTC TGG ATG GAG CA  
*Prmt5 R* GCA TCT CAA ACT GTG CCT CA  
*Prmt6 F* AAA CCT CTG GTG CTG TCC AC  
*Prmt6 R* CCG GAA ATG TCC GTA TCT TG  
*Prmt7 F* GCA CAA TGG AGC TGA CAA GA  
*Prmt7 R* GAT CGT GCT GTC TGG AGT GA  
*Prmt8 F* TGG AGG GCT TAT GTT TCC AG  
*Prmt8 R* AAG GAC AGC TCT TCC GTC TTC  
*Prmt9 F* AGC ACA TGC ACA GTT GGT TC  
*Prmt9 R* ACC CAA ATC CCA GCT AAC G  
*Rfx3 F* CAC ATC GCT CAA TCA CCT GG  
*Rfx3 R* GCT GCA GGG TCA TCT TGA AG  
*Setbp1 F* AGT TGG CCT TGA AAC AGG TG  
*Setbp1 R* GAG GTT TGG CCT TGC TAC AC  
*Srcin1 F* ACG TGA AGC CAG ATG AGG AC  
*Srcin1 R* AGC GGA GTA GGT GCT GAG AG  
*Usp46 F* ACC AGC CGA GAA CAA TAA GC  
*Usp46 R* ACA GCG TTT CTG TGT TGC TG

<b>Ab name</b>	<b>Source</b>	<b>Catalog number</b>
Actin	millipore	8691002
FAK(C-20)	santa cruz	sc558
GAPDH	cell signaling	2118
GFP	aves	1020
H3	abcam	1791
H3R2me2a	millipore	04-808
H3R2me2s	Guccione's gift	
H3R8m2a	active motif	39651
H4R3me2a	abcam	129231
H4R3me2s	abcam	5823
p-FAK (Y397)	biosciences	611722
p-FAK (Y925)	santa cruz	sc11766
p-Src (Y517)	cell signaling	2105
p-Src (Y416)	cell signaling	6943
PRMT1	abcam	73246
PRMT5	abcam	31751
PRMT6	bethyl	A300-929A
PRMT7	abcam	22110
Src(32G6)	cell signaling	2123
Srcin1	Defilippi's gift	